Systematic investigation of α- and cluster-decay modes in superheavy nuclei

M. Ismail,[1] S. G. Abd-Elnasser,[2] A. Adel ®,[1,*] I. A. M. Abdul-Magead ®,[1] and H. M. Elsharkawy ®[2]

[1]*Physics Department, Faculty of Science, Cairo University, 12613 Giza, Egypt*

[2]*Physics Department, Faculty of Science, Fayoum University, 63514 Fayoum, Egypt*

We systematically investigate the α-decay and spontaneous fission (SF) half-lives of superheavy nuclei (SHN) $Z = 124$ and 126 in the mass number range $292 \leqslant A \leqslant 314$. The α-decay half-lives ($\log_{10} T_{1/2}$) have been calculated within the double folding model (DFM), the universal decay law (UDL), the scaling law of Horoi, and the universal curve (UNIV) formula. To identify the mode of decay of these SHN, a competition between SF half-lives and α-decay half-lives has been performed. The study reveals that even-mass number isotopes of $^{292-314}124$ and $^{292-314}126$ will survive fission, and α chains can also be predicted from these SHN. The variation of $\log_{10} T_{1/2}$ against parent nucleus mass numbers of α-decay chains of each SHN isotope is found to be governed by the presence of magic or semimagic nucleon numbers of the parent nucleus in the sense that $\log_{10} T_{1/2}$ becomes maximum at or near these numbers. The probable heavy cluster radioactivity (CR) in the mass number range $A_c = 18$–126 from $^{294-324}124$ and $^{294-312}126$ is also studied using the same four models of α-decay half-lives. Heavy clusters with charge numbers in the range $36 \leqslant Z_c \leqslant 46$ are dominant decay modes relative to α decay. Clusters with small $\log T_c$ values relative to α decay are found to be the six clusters, Kr, Sr, Zr, Mo, Ru, and Pd. The most probable cluster emissions having the smallest $\log T_c$ values relative to α decay are $^{104-106}$Mo and $^{106-110}$Ru from $^{312}124$; from $^{296}126$ the clusters are $^{94-96}$Mo, $^{104-106}$Pd; from $^{298}126$ the clusters are ^{90}Zr, ^{96}Mo; and from the SHN isotope $^{300}126$ the most probable clusters are $^{100-102}$Ru. We found that the most probable cluster emissions occur when the proton and neutron numbers in the emitted clusters and their residual daughter nuclei are magic or near to the magic numbers.

I. INTRODUCTION

The investigation of the "island of stability" in the superheavy region and the synthesis of new superheavy nuclei (SHN) has become a topic of considerable interest within the nuclear physics community [1–8]. The quantum shell effects and the notable shell gaps that could exist in SHN are essential for their stability. These effects have a major impact on the formation of a sizable barrier against their spontaneous fission. Investigating the properties of these superheavy elements (SHEs) expands our fundamental understanding of various nuclear structure aspects, such as decay modes, shell closures, nuclear deformation, nuclear spin, and nucleus-nucleus interactions. The predicted existence of an island of stability arises within this interesting domain, characterized by SHN exhibiting magic numbers of both protons and neutrons. Surrounding this island, however, are short-lived nuclei that compose a sea of instability, marking the boundaries of this domain. As we get closer to the core of the island of stability, the emergence of the expected magic neutron number, $N = 184$, becomes increasingly apparent, while the predicted presence of the proton magic number between $Z = 114$–126 remains a subject of exploration [1,9].

The seventh period of the periodic table of elements reached its completion with the addition of four newly discov-ered superheavy elements (SHEs). These elements, namely nihonium ($Z = 113$), moscovium ($Z = 115$), tennessine ($Z = 117$), and oganesson ($Z = 118$), have now become essential elements of the periodic table. The synthesis of SHN is performed using heavy-ion fusion reactions utilizing two distinct fusion evaporation mechanisms. The first approach employs cold fusion reactions, utilizing closed shell targets of ^{208}Pb or ^{209}Bi in combination with various projectiles of medium-mass stable isotopes of Ti, Cr, Fe, Ni, and Zn. Notably, this method was implemented at GSI (Darmstadt) and RIKEN (Wako) [10,11]. It has succeeded in synthesizing SHEs with $Z = 107$–113. The second mechanism involves hot fusion reactions, where doubly magic neutron rich ^{48}Ca projectiles are directed at actinide targets. This approach proved successful in synthesizing superheavy nuclei with atomic numbers ranging from 112 to 118, and was conducted at esteemed research laboratories including JINR-FLNR (Dubna) and LBNL (Berkeley). Currently, the heaviest known element synthesized is $^{294}_{118}$Og (with a half-life of $0.89^{+1.07}_{-0.31}$ ms), achieved through the ^{48}Ca $+ ^{249}$Cf hot fusion reaction [12]. Despite the successful synthesis of superheavy nuclei as heavy as ^{294}Ts ($Z = 117$) and ^{294}Og ($Z = 118$), which possess 177 and 176 neutrons respectively, these isotopes were 7 and 8 neutrons less than the closed shell $N = 184$. Hence, the central region of the long-sought island of stability remains undiscovered. In a recent study [13], researchers conducted a search for the production of superheavy elements with atomic numbers 119 and 120. They used fusion-evaporation reactions ^{50}Ti $+ ^{249}$Bk

*ahmedadel@sci.cu.edu.eg

and ^{50}Ti + ^{249}Cf. The experiment lasted for four months of irradiation. However, the researchers were unable to detect the presence of elements 119 and 120 at the given cross-section sensitivity levels of 65 and 200 fb for the ^{50}Ti + ^{249}Bk and ^{50}Ti + ^{249}Cf reactions, respectively. Currently, there are ongoing experiments aimed at creating superheavy nuclei (SHN) with atomic numbers greater than 118. However, these experiments face notable challenges due to limitations in beam intensity, availability of suitable targets, and the low production cross section, which is measured in picobarn and below. As a result of these experimental constraints, theoretical predictions play a vital role as they provide a valuable tool for exploring the boundaries and possibilities within this region.

Superheavy nuclei usually undergo consecutive α-decay chains, that eventually ends in spontaneous fission. Newly synthesized superheavy nuclei (SHN) can be identified by analyzing the decay products of α-decay chains. There is another type of decay known as cluster radioactivity, which follows the same mechanism as α decay. According to the research of Poenaru *et al* [14–16], it is proposed that cluster decay could potentially compete with α decay and spontaneous fission in certain isotopes of superheavy nuclei. This implies that, for specific SHN, cluster decay may be an alternative decay mode alongside α decay and spontaneous fission.

Numerous theoretical approaches have been proposed to effectively explain cluster radioactivity (CR). These models can be categorized into two main groups: the fissionlike model and the clusterlike model. In the fissionlike approach, the nucleus undergoes a continuous deformation process, assuming various geometrical shapes. The cluster is believed to gradually form during the adiabatic rearrangements of parent nuclei until the scission configuration is reached. On the other hand, the clusterlike model, which resembles α decay, is a nonadiabatic method. In this model, the cluster is preformed with a certain preformation probability within the decaying parent nucleus, and it subsequently penetrates through the Coulomb barrier. Various theoretical approaches have been developed to effectively explain α decay and cluster radioactivity. These approaches include the generalized liquid-drop model [17,18], the density-dependent cluster model [6,7,19–22], the fissionlike model [4,15,16], and the Coulomb and proximity potential model (CPPM) [23–26]. In addition to these models, several empirical formulas have been developed to reproduce experimental data for cluster decays. These include the universal decay law (UDL) [27,28], the universal curve (UNIV) [29], the Horoi formula [30], and the unified description formula (NRDX) [31]. The complete microscopic treatment of α decay and cluster radioactivity poses a challenging and intricate quantum-mechanical problem. Over the past century, numerous microscopic models have been developed to describe these decay processes. Qi *et al.* [32] have presented a comprehensive review of recent advancements in the understanding of radioactive particle decay, encompassing both experimental and theoretical progress in this field. Warda *et al.* [33], from a microscopic standpoint, have examined the cluster emission characteristics of a wide range of even-even actinide nuclei spanning from ^{222}Ra to ^{242}Cm. Their study employed the mean-field Hartree-Fock-

Bogoliubov theory along with the phenomenological Gogny interaction. Xu *et al* [34] presented a microscopic calculation of α-cluster formation in heavy nuclei by employing the quartetting wave function approach (QWFA), which was inspired by the successful application of the THSR (Tohsaki-Horiuchi-Schuck-Röpke) wave function concept to light nuclei. Yang *et al.* [35] utilized the QWFA to perform a microscopic calculation of α-cluster formation and decay in ^{104}Te, ^{212}Po, and their neighboring nuclei. In a recent study by Wang and Ren [36], the impact of surface polarization on cluster radioactivity within the trans-lead region was investigated. They employed an improved density-dependent cluster model that thoroughly considered nuclear deformation. They introduced a novel, unified representation of deformation-dependent diffuseness in the nuclear density distribution by introducing an adjustable parameter. This parameter's sign determined the specific surface polarization mode, and its amplitude, along with deformation parameters, handles the degree of surface polarization in deformed nuclei.

This study focuses on investigating the α-decay chains of various isotopes of superheavy elements (SHEs) with $Z = 124$ and 126, which have not yet been synthesized. The α-decay half-lives are computed using the density-dependent cluster model. The penetration probability is calculated using the WKB approximation, applying the Bohr-Sommerfeld quantization condition. The computed half-lives of the decay chains for the SHE isotopes with $Z = 124$ and 126 are compared with other empirical formulas. Furthermore, the dominant decay mode of these isotopes and their α-decay chains is determined by comparing the α-decay half-lives with the half-lives of spontaneous fission. Additionally, the feasibility of cluster emission from several superheavy isotopes is investigated using various theoretical approaches. The predictions made in this particular region of superheavy nuclei hold potential significance for future experimental explorations in this field.

The structure of the article is outlined as follows. In the subsequent section, we provide an overview of the general theoretical framework used to calculate the half-lives of α and cluster decays. Section III is dedicated to the analysis and discussion of the results obtained. Finally, a summary and conclusion are presented in Sec. IV.

II. THEORETICAL FRAMEWORK

A. Universal decay law (UDL) formula

Based on the *R*-matrix theory, Qi *et al.* [27,28] derived a linear universal decay law (UDL) that describes the microscopic mechanism of charged-particle emission, applicable to both α and cluster decays. In this study, we utilize the universal decay law (UDL) formula, which is expressed as follows:

$$\log_{10}(T_{1/2}) = a Z_c Z_d \sqrt{\frac{\mu}{Q_c}} + b \sqrt{\mu Z_c Z_d \left(A_d^{1/3} + A_c^{1/3}\right)} + c,$$

(1)

Here, μ is defined as $\mu = A_c A_d/(A_c + A_d)$, where A_d represents the mass number of the daughter nucleus and A_c corresponds to the mass number of the emitted cluster. The

released energy of the cluster decay, denoted as Q_c, is calculated based on the mass excess of the nuclei involved [37]. In the above equation, the coefficients for the UDL formula are as follows: $a = 0.3949$, $b = -0.3693$, and $c = -23.7615$.

B. The universal curve (UNIV)

Poenaru *et al.* [29] proposed that a single line on the universal (UNIV) curve for α-decay and cluster radioactivities is established by plotting the sum of the decimal logarithms of half-life and cluster preformation probability against the decimal logarithm of external barrier penetrability as

$$\log_{10} T_{1/2} = a(\mu Z_c Z_d R_b)^{1/2} \times [\arccos \sqrt{r} - \sqrt{r(1-r)}]$$
$$+ b(A_c - 1) + [\log_{10}(\ln 2) - \log_{10} \nu_0], \quad (2)$$

where $r = R_t/R_b$, R_t and R_b represent the first and second turning points of the barrier, in which they can be given by $R_t = 1.2249(A_d^{1/3} + A_c^{1/3})$ and $R_b = 1.43998 Z_d Z_c/Q$. The assault frequency ν_0 is taken as $10^{22.01}$ s^{-1} [38]. The constants thus used here are $a = 0.22873$ and $b = 0.598$.

C. Spontaneous fission half-lives

Xu *et al.* introduced a semiempirical approach for estimating half-lives of spontaneous fission (SF), formulated as follows [39]:

$$T_{1/2} = \exp\left\{2\pi\left[C_0 + C_1 A_p + C_2 Z_p^2 + C_3 Z_p^4 \right.\right.$$
$$\left.\left. + C_4(N_p - Z_p)^2 - \left(0.13323\frac{Z_p^2}{A_p^{1/3}} - 11.64\right)\right]\right\}. \quad (3)$$

The constants are $C_0 = -195.09227$, $C_1 = 3.10156$, $C_2 = -0.04386$, $C_3 = 1.4030 \times 10^{-6}$, and $C_4 = -0.03199$.

D. The cluster decay within the density-dependent cluster model

Within the context of the density-dependent cluster model, the parent nucleus can be conceptualized as a two-body system, comprising the cluster and the daughter nucleus, interacting with each other. The comprehensive interaction potential of the cluster-core system encompasses the attractive nuclear potential, repulsive Coulomb potential, and the centrifugal component, and can be expressed as follows:

$$V_T(R) = \lambda V_N(R) + V_C(R) + \frac{\hbar^2}{2\mu}\frac{\left(\ell + \frac{1}{2}\right)^2}{R^2}, \quad (4)$$

Here, R denotes the distance between the centers of mass of the cluster and the core. The renormalization factor λ in Eq. (4) accounts for the adjustment of the nuclear potential through the application of the Bohr-Sommerfeld quantization condition [40,41]. μ corresponds to the reduced mass of the cluster-daughter system. The final term in Eq. (4) represents the modified centrifugal potential, as corrected by Langer [42]. The angular momentum ℓ carried by the emitted cluster follows the spin-parity selection rule, with the assigned spin-parity values for the ground states of the relevant nuclei obtained from Ref. [43].

The nuclear and Coulomb potentials can be derived using the double-folding model, as described in previous studies [44,45]:

$$V_{N(C)}(R) = \int d\vec{r}_1 \int d\vec{r}_2 \, \rho_c(\vec{r}_1) \, \upsilon_{N(C)}(s) \, \rho_d(\vec{r}_2). \quad (5)$$

In the above equation, $\vec{s} = \vec{r}_2 - \vec{r}_1 + \vec{R}$ represents the relative distance between a constituent nucleon in the emitted cluster and a nucleon in the daughter nucleus, where $\vec{r}_1$ and $\vec{r}_2$ denote their respective positions, and $\vec{R}$ represents the separation vector between the centers of mass of the cluster and the daughter nucleus. The term $\upsilon_C(s)$ corresponds to the Coulomb force between protons, which follows the standard proton-proton Coulomb interaction. For the effective nucleon-nucleon (*NN*) interaction, denoted as $\upsilon_N(s)$, we employ the widely used Michigan three-range Yukawa (M3Y)-Reid-type interaction, which includes a zero-range exchange contribution [44]:

$$\upsilon_N(s) = \left[7999\frac{e^{-4s}}{4\,s} - 2134\frac{e^{-2.5s}}{2.5\,s}\right]$$
$$- 276\left[1 - 0.005\left(\frac{E_c}{A_c}\right)\right]\delta(\vec{s}). \quad (6)$$

In Eq. (6), E_c is the kinetic energy of the cluster, given by $E_c = Q_c A_d/(A_c + A_d)$. The last term in Eq. (6) accounts for the knock-on exchange effect and is incorporated using a zero-range pseudopotential.

The matter and charge density distributions of nuclei are represented using the commonly employed two-parameter Fermi (2pF) form, given by

$$\rho(r) = \frac{\rho_0}{1 + \exp\left(\frac{r - R_0}{a}\right)}. \quad (7)$$

The value of ρ_0 is determined by integrating the matter (or charge) densities equivalent to the mass number (or atomic number) of the nucleus. The half-density radius, denoted as R_0, and the diffuseness parameter, represented by a, are defined as follows (given by [46]):

$$R_0 = 1.07 A_d^{1/3} \text{ fm}, \quad a = 0.54 \text{ fm}. \quad (8)$$

The renormalization factor λ of the nuclear potential, as given by Eq. (4), can be computed by applying the Bohr-Sommerfeld quantization condition [40,41], which is expressed as

$$\int_{R_1}^{R_2} dr \, k(r) = (G - \ell + 1)\frac{\pi}{2}, \quad (9)$$

where $k(r) = \sqrt{2\mu |V_T(r) - Q_c|/\hbar^2}$ is the wave number. R_i ($i = 1, 2, 3$) are the three turning points for the cluster-daughter potential barrier, where $V_T(r)|_{r=R_i} = Q_c$. The global quantum number G is determined from the Wildermuth and Tang condition [47]. It can be represented as [47–50]

$$G = \sum_{i=1}^{A_c} \left(g_i^{(A_c + A_d)} - g_i^{A_c}\right),$$

where $g_i^{(A_c + A_d)}$ are the oscillator quantum numbers of the nucleons forming the cluster, whose values are required to

guarantee the cluster is completely outside the shell occupied by the core nucleus, and $g_i^{(A_c)}$ are the interior quantum numbers of the A_c nucleons for the cluster in the shell model [7,21,50]. We take the values of oscillator quantum numbers g_i as in Refs. [7,21,50].

The computation of the cluster decay half-life is given by the following expression [49,51]:

$$T_{1/2} = \frac{\hbar \ln 2}{S_c \, \Gamma_c}, \tag{10}$$

The quantum penetration probability, P_c, and the knocking frequency, ν_c, of the emitted cluster can be computed within the WKB approximation. Using this approximation, the cluster decay width Γ_c is given by $\Gamma_c = \hbar \nu_c P_c$. The preformation probability of the cluster inside the parent nucleus is denoted as S_c. The expressions for P_c, ν_c, and S_c can be found in Refs. [41,49,51]:

$$\nu_c = \left[\int_{R_1}^{R_2} \frac{2\,\mu}{\hbar\, k(r)}\, dr \right]^{-1} \tag{11}$$

and

$$P_c = \exp\left(-2 \int_{R_2}^{R_3} k(r)\, dr \right). \tag{12}$$

In our calculations of the cluster decay half-life, we employ the exponential formula for the preformation probability S_c, as proposed in Refs. [31,50]:

$$\log_{10} S_c = a\sqrt{\mu\, Z_c\, Z_d} + b, \tag{13}$$

where Z_c (Z_d) is the atomic number of the emitted cluster (daughter nucleus). The parameters a and b of the formula given by Eq. (13) are obtained from Ref. [50] with the values $a = -0.052$, $b_{e-e} = 0.690$, and $b_{o-A} = -0.600$.

E. α decay within the density-dependent cluster model

The density-dependent cluster model is considered one of the successful theoretical frameworks for describing various types of nuclear decay processes, including cluster radioactivity and α decay [19,46,52–55]. We can employ the same methodology of the density-dependent cluster model, as applied to cluster decay, for α decay, with some variations and additional considerations pertaining to the specific parameter choices used in the α-decay calculations. In calculating the nuclear potential for α decay, the matter density distribution of the cluster, denoted as ρ_c, in Eq. (5), which is represented by two-parameter Fermi form, is replaced by the density distribution of the α particle, denoted as ρ_α, and represented as

$$\rho_\alpha(r_1) = 0.4229 \exp\left(-0.7024 r_1^2\right), \tag{14}$$

whose volume integral is equal to the mass number of the α particle. The matter density distribution for the daughter nucleus can be described by the two-parameter Fermi form of Eq. (7). The values of global quantum number G, as employed

in Eq. (9), in the case of α-decay can be expressed as [40,52]

$$G = \begin{cases} 20 & \text{for } (N > 126), \\ 18 & \text{for } (82 < N \leqslant 126), \\ 16 & \text{for } (N \leqslant 82). \end{cases} \tag{15}$$

The α-preformation factor S_α of the α particle can be estimated, as a function of the shell and subshell closures (Z_0, N_0) of the parent nucleus and the number of protons $(Z - Z_0)$ and neutrons $(N - N_0)$ outside them, by the phenomenological formula given in Ref. [56] as

$$S_\alpha = \mathcal{A}\frac{e^{-0.003(Z-Z_0-Z_c)^2} e^{-0.006(N-N_0-N_c)^2} - a_p}{a_l}. \tag{16}$$

For the region of nuclei considered here, the adopted values for the parameters $\mathcal{A}(Z_0, N_0)$, Z_c, and N_c for different shell closures (Z_0, N_0) are taken from Refs. [56–58]. Z_c (N_c) defines the number of protons (neutrons) outside the shell closures (Z_0, N_0).

III. RESULTS AND DISCUSSION

For superheavy nuclei (SHN), α-decay and spontaneous fission (SF) are the mainly favored decay modes. In this work, we calculated the α-decay and spontaneous fission half-lives for superheavy nuclei $^{292-314}124$ and $^{292-314}126$ to identify the most probable mode of decay of these nuclei. The SF half-lives were calculated using the semiempirical formula given by Xu *et al* [39]. However, we conducted the calculation of α-decay half-lives using the double-folding model (DFM), which is derived from the Michigan three-range Yukawa-Reid *NN* interaction. Additionally, we employed three empirical formulas: UDL [27,28], UNIV [29], and the Horoi formula [30,38], to predict α-decay half-lives. The results of these computations within the specified theoretical frameworks are presented in Figs. 1–3 for $Z = 124$ and Figs. 4–6 for $Z = 126$. Furthermore, it is noteworthy that the α-decay half-lives obtained from the UDL, Horoi, and UNIV formulas exhibit a good agreement with our theoretical calculations based on the DFM. Figures 1–3 depict a graphical representation of $\log_{10} T_{1/2}$ plotted against the mass number of the parent nuclei. This graphical representation enables a comparative analysis of the calculated α-decay and spontaneous fission (SF) half-lives for isotopes $^{292-312}124$ and their respective α-decay products. Figure 1(a) shows that the elements $^{292}124$, $^{288}122$, $^{284}120$, $^{280}118$, $^{276}116$, and $^{272}114$ have α-decay half-lives less than the corresponding SF half-lives. Thus, the isotope $^{292}124$ survives fission and shows 6α chains from this isotope. Figures 1(b), 1(c) and 1(d) show that the isotopes $^{294}124$, $^{296}124$ and $^{298}124$ survive fission and respectively predict 7α, 8α and 8α chains from the three isotopes. Figure 2 shows that the isotopes $^{300-306}124$ will survive fission and show 8α chains from each of the three isotopes $^{300-304}124$ and 5α chains from $^{306}124$ isotope. Figure 3 depicts the decay properties of $^{308-314}124$ isotopes. It is evident from this figure that these isotopes will survive fission, and 5α, 4α, and 3α chains can be predicted, respectively, from the isotopes $^{308}124$, $^{310-312}124$, and $^{314}124$. Figures 4–6 show the same as Figs. 1–3 but for the SHN $Z = 126$. Figure 4 shows that the isotopes $^{292-298}126$ survive fission and 5α,
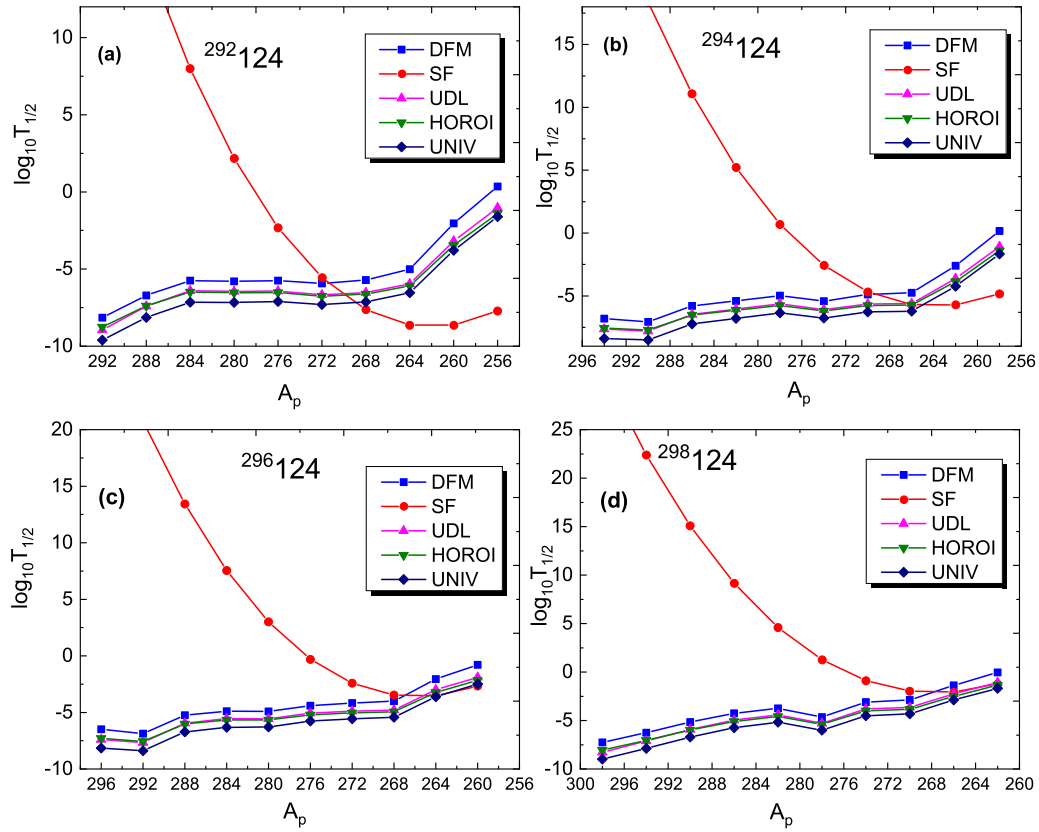
FIG. 1. Comparison of the calculated α-decay half-lives of the isotopes $^{292-298}124$ and products on their α-decay chains.
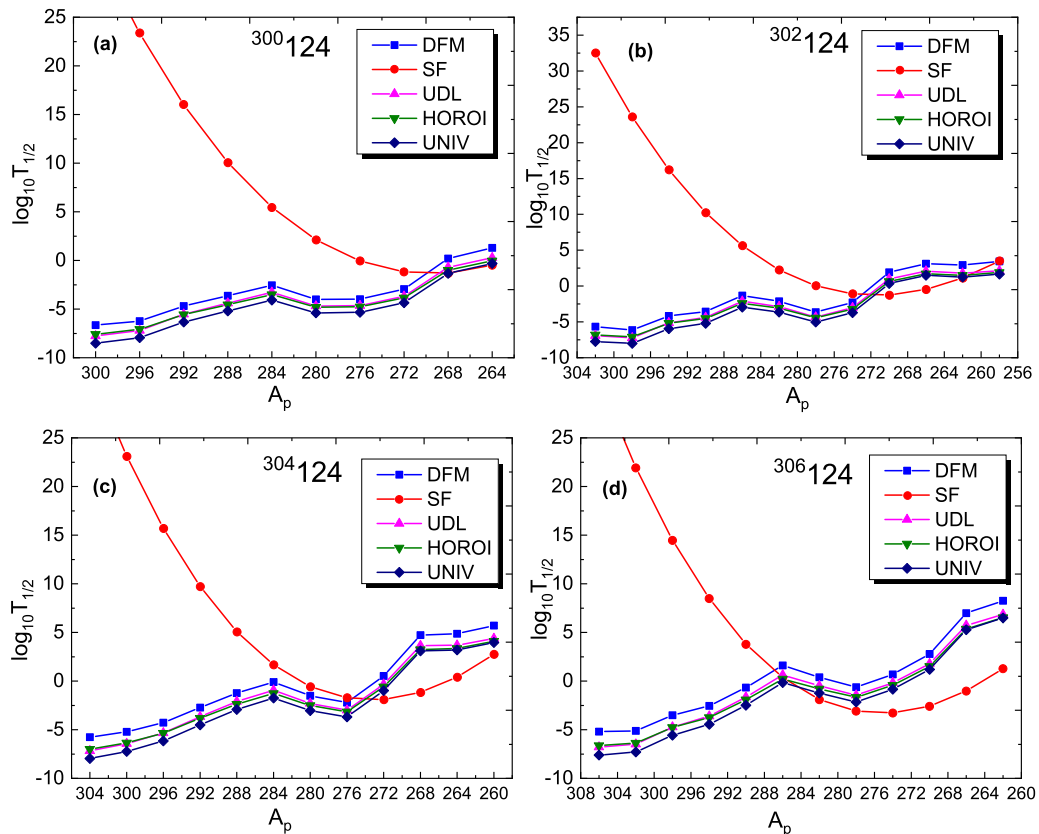
FIG. 2. The the same as Fig. 1 but for $^{300-306}124$ isotopes.
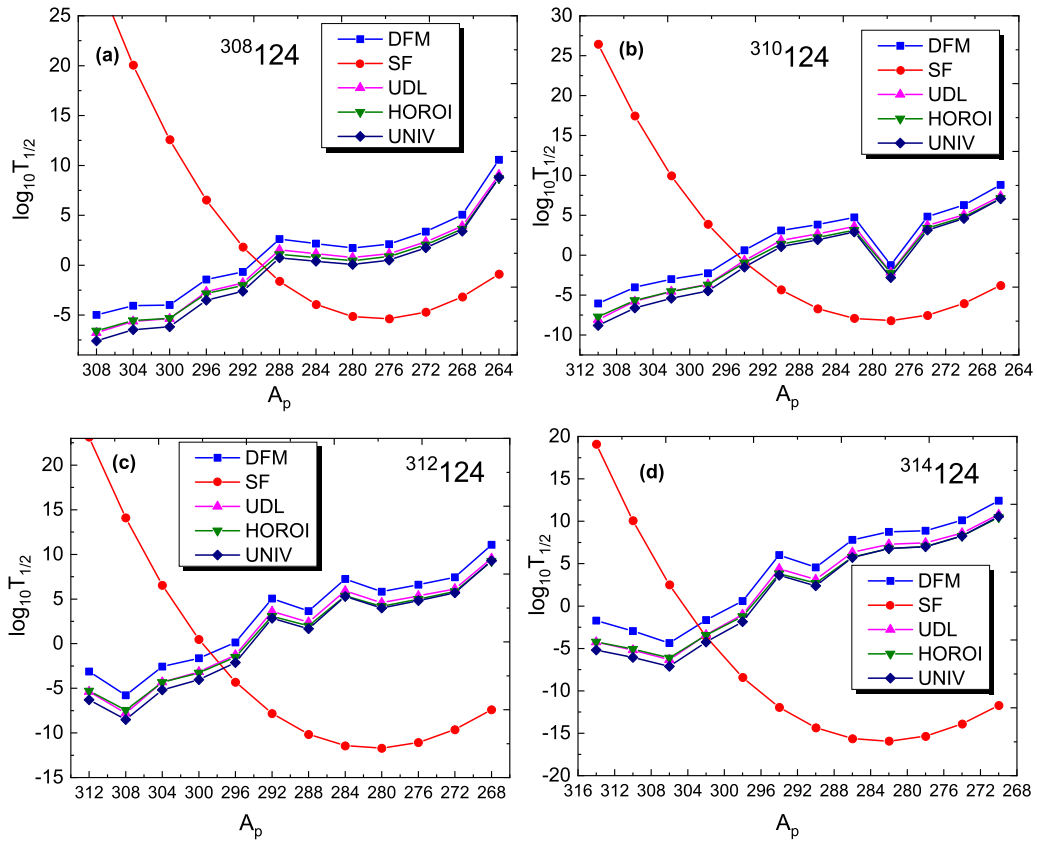
FIG. 3. The the same as Fig. 1 but for $^{308-314}124$ isotopes.
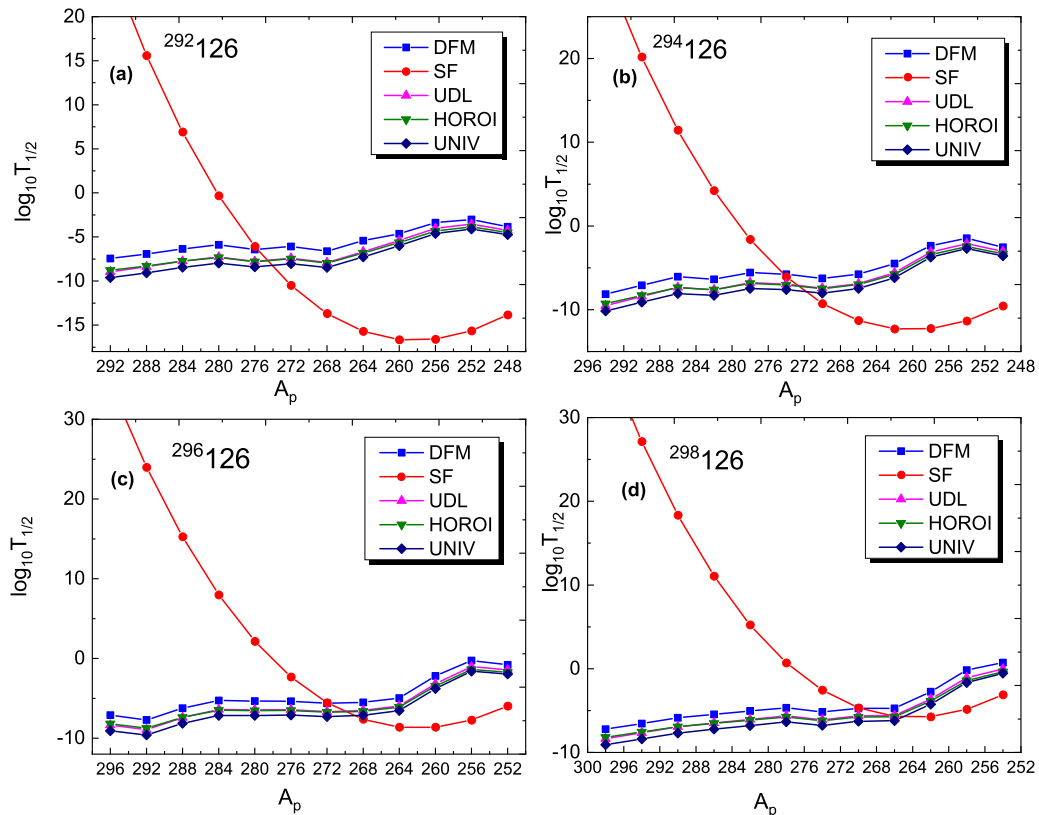
FIG. 4. Comparison of the calculated α-decay half-lives of the isotopes $^{292-298}126$ and products on their α-decay chains.
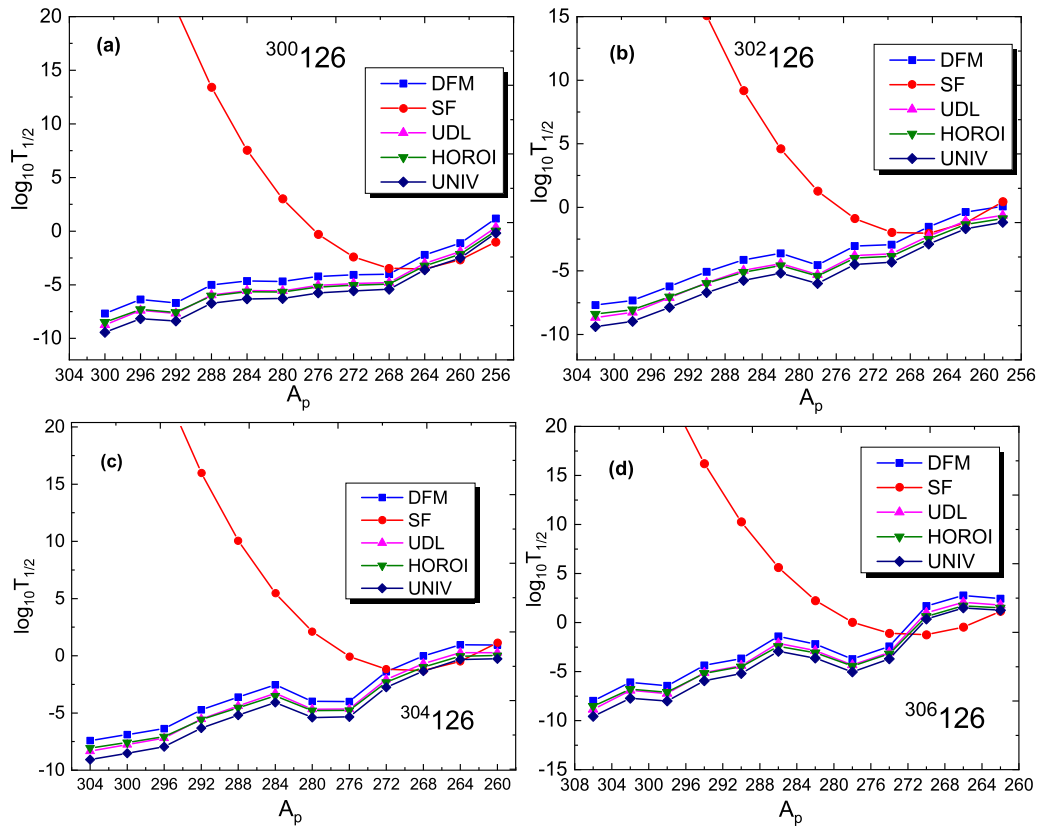
FIG. 5. The the same as Fig. 4 but for $^{300-306}126$ isotopes.
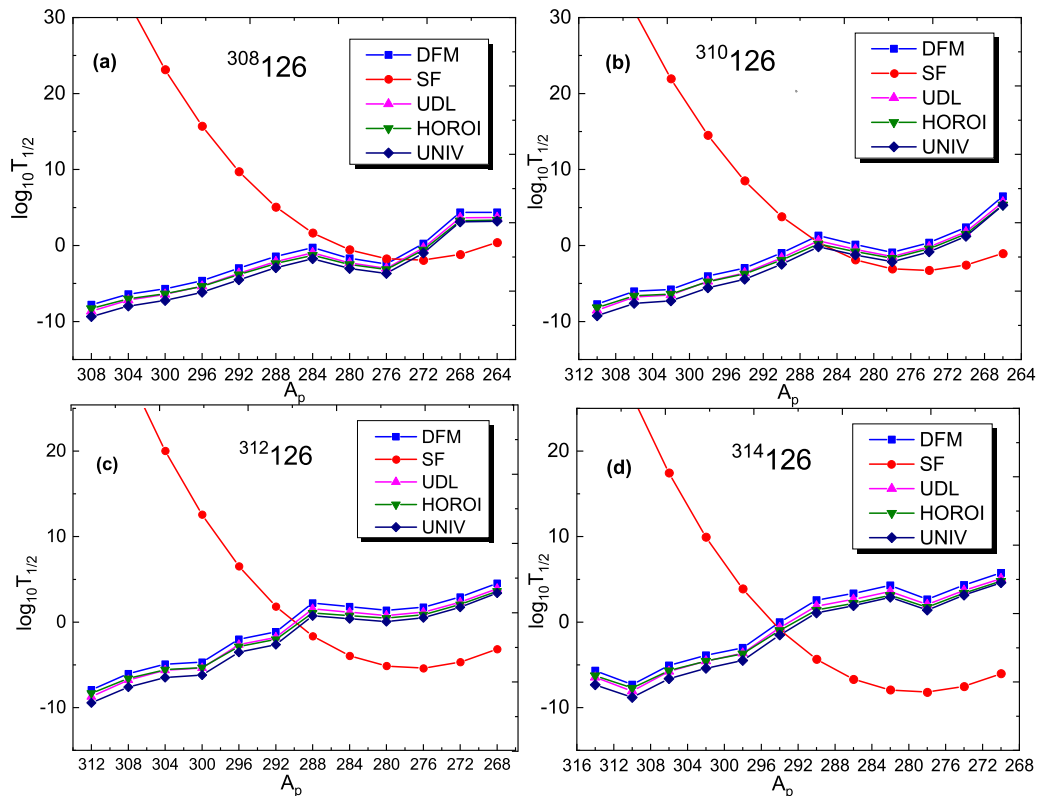
FIG. 6. The the same as Fig. 4 but for $^{308-314}126$ isotopes.

6α, 7α, and 8α chains are expected, respectively, from the isotopes $^{292}126$, $^{294}126$, $^{296}126$, and $^{298}126$. In Fig. 5, it can be noted that the isotopes $^{300-306}124$ survive fission and 9α chains are predicted from each isotope. Figure 6 displays that the $^{308-314}126$ isotopes will survive fission, and 9α, 6α, and 5α chains can be expected, respectively, from the isotopes $^{308}126$, $^{310-312}126$, and $^{314}126$.

It is assumed that the stability of the parent nuclei is proportional to the height of the maximum value in $\log_{10} T_{1/2}$, a relationship influenced by the existence of neutron and/or proton magic or semimagic numbers. At nucleon magic numbers, the nucleus becomes more stable against α decay and $T_{1/2}$ increases. By examining the obtained half-lives in Fig. 1, it can be seen that α-decay chains of $^{292-298}124$ isotopes have maxima at $(Z_p, N_p) = (120, 164)$, $(116,162)$, and $(116,166)$, for the isotopes $^{292}124$, $^{294}124$, and $^{298}124$, respectively. For the isotopes $^{296}124$ in Fig. 1(c), no maximum value of $\log_{10} T_{1/2}$ appears. Given that, the proton numbers $Z = 116$ and 120 are predicted as proton magic numbers [49,59–62] and the neutron number $N = 162$ is a neutron magic number [59,61,63–65] beyond the magicity $N = 152$. This convergence in our prediction and those of other researchers underscores the agreement in the identification of magic numbers. Figures 2(a)–2(d) have clear maxima at proton and neutron numbers of parent nuclei $(116,168)$ for the $^{300}124$ isotope, at $(116,170)$ for the $^{302}124$ isotope, at $(114,170)$ for the $^{304}124$ isotope, and clear and sharp maximum at $(114,172)$ for the $^{306}124$ element. These values of maxima in α-decay half-lives values can be explained by their magical or semimagical behavior of proton and neutron numbers of $^{300-306}124$ isotopes. It can be seen that the proton numbers in the parentheses are equal to the proton magicities $Z = 114$ and 116 [60,61,66]; also the neutron numbers differ slightly or are equal to the neutron magicity $N = 172$ [60,61,66]. Figures 3(a) and 3(b) show the α-decay chains compared to the SF process for isotopes $^{308-310}124$. These figures depict the presence of a local maximum at $(Z_p = 114, N_p = 174)$ for the isotope $^{308}124$, and at $(Z_p = 110, N_p = 172)$ for the isotope $^{310}124$. In the case of the $^{312}124$ isotope, there are two local and sharp maxima at $(Z_p, N_p) = (114, 178)$ and $(110,174)$. Given that, $Z = 110, 114$ and $N = 178$ were predicted as magic or semimagic numbers [67,68]. Figure 3(d) shows the α-decay chains of element $^{314}124$, it has a clear maximum at $(114,180)$, which indicates the magical or semimagical behavior of these Z_p and N_p. It is worth noting that the neutron energy level spectra for superheavy nuclei with proton numbers $Z = 114$ and 120, as outlined in Refs. [61,69,70], predict $N = 184$ as a neutron magic number. The neutron gap of this number has $3d_{3/2}$ and $3s_{1/2}$ levels at the top of the gap. As these two levels become unoccupied, they give rise to the appearance of the two neutron semimagic numbers, specifically $N = 180$ and 178.

The calculated half-lives in Fig. 4 show that the α-decay chains of $^{292-298}126$ isotopes. As can be seen in these figures, there exist clear maxima at $(Z_p = 106, N_p = 148)$ for the isotope $^{294}126$ and at $(Z_p = 106, N_p = 150)$ for the isotope $^{296}126$. In Fig. 5, there exist clear maxima in both Figs. 5(c) and 5(d) at $Z_p = 116$ and neutron numbers of the parent nuclei $N_p = 168$ and 170 for $^{304}126$ and $^{306}126$, respectively.

Figures 6(a)–6(d) show the α-decay chains compared to the SF process for isotopes $^{308-314}126$. As can be seen in these figures, there exist clear maxima at $(Z_p = 114, N_p = 170)$ for the isotope $^{308}126$, at $(Z_p = 114, N_p = 172)$ for the isotope $^{310}126$, and at $(Z_p = 114, N_p = 174)$ for the isotope $^{312}126$. These maxima are considered as an indication of the magical or semimagical behavior of these Z_p and N_p.

The preceding discussion points out that, when plotting the variation of $\log_{10} T_{1/2}$ against the mass numbers of parent nuclei in the α-decay chains of superheavy nuclei (SHN), distinctive peaks (maxima) in $\log_{10} T_{1/2}$ appear at specific combinations of proton and neutron numbers. These particular numbers correspond to magic proton numbers (e.g., $Z_P = 114$), or magic neutron numbers (such as $N_P = 184$), or even nucleon numbers near magicity (like $Z_P = 106$ and 116 and $N_P = 150, 164, 170, 174$, and 178).

It is known that decay energies of the outgoing cluster play a crucial role in determining the half-lives of the emitted particles. So, it is important to perform the calculations of half-lives using α-decay energies derived from accurate mass model. According to a comparison between the calculated results and the experimental data, it was shown in Ref. [71] that the WS4 mass model is the most accurate one to reproduce the experimental Q_α values of SHN. It is interesting to show whether our conclusions on the prediction of magic numbers still hold when alternate mass models are employed. Figure 7 shows α-decay chains of the SHN isotope $^{298}124$ calculated using WS3 + RBF [72], WS3 [73], and KTUY [74] mass models. The maximum of $\log_{10} T_{1/2}$ for the three graphs is at $(Z_p, N_p) = (118, 168)$ which differs by one α-decay compared to the results of WS4 mass model. For the first two mass models, $\log_{10} T_{1/2}$ for the point $(116,166)$ has almost the same value as the maximum point. The proton number $Z_p = 118$ can be submagic since the levels $2f_{5/2}$ and $3p_{3/2}$ are above the proton magicity $Z = 114$ in the theoretical calculations of the proton level scheme for $Z = 114, 120$, and 126 studied in Ref. [62]. When $2f_{5/2}$ is filled first, it produces the magicity 120 and if $3p_{3/2}$ is filled first it produces the submagicity 118. Figure 8 is the same as Fig. 7 but for the isotopes $^{306}124$. The maximum in the three graphs are at $(116,166)$ as in the WS4 mass model. This means that, for this large mass number, the three mass models predict the same results as the WS4 model.

In addition to α decay and SF, cluster radioactivity (CR) is also a possible decay mode of SHN. Poenaru *et al.* [15,75] predicted that the CR half-lives for some superheavy nuclei show a trend towards shorter half-lives relative to α decay. This prediction implies the possibility of cluster decay with half-lives denoted as T_c, which could be comparable to or even shorter than the T_α half-lives. For example, if $\log_{10}(T_\alpha/T_c)$ has positive value for certain cluster, this means that T_c is small compared to T_α and the SHN decay by emitting this cluster. Also, if $\log_{10}(T_\alpha/T_c)$ is a small negative value, say -0.9, it means that the half-life time for cluster emission is eight times greater compared to T_α. Thus, the competition between α decay and CR can be compared by the quantity $\log_{10} b_c = \log_{10} T_\alpha - \log_{10} T_c$, which is called the branching ratio of CR relative to the corresponding α decay. If $\log_{10} b_c > 0$, it means that CR is the dominant decay mode relative to α
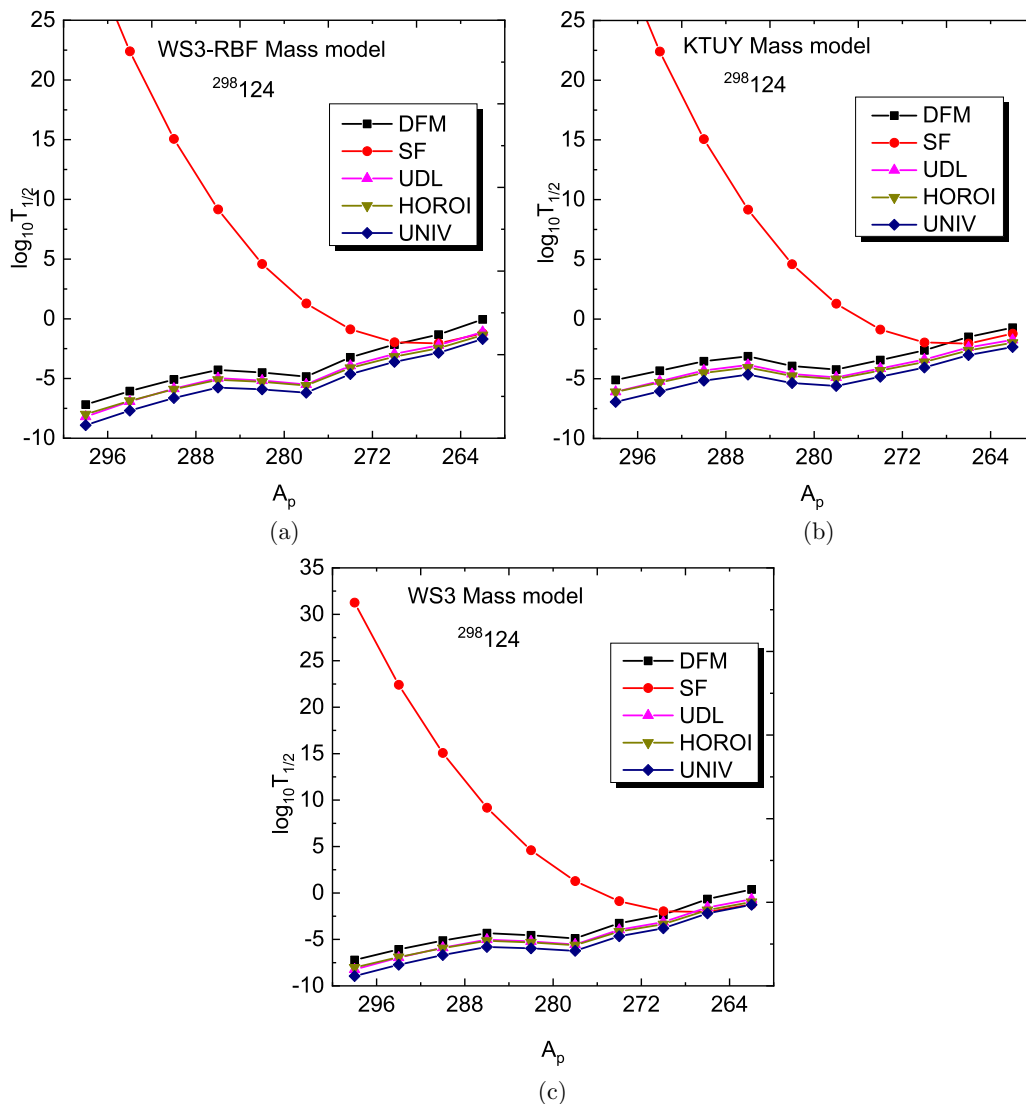
FIG. 7. Comparison of the calculated α-decay half-lives of the isotope $^{298}124$ and products on their α-decay chains using different mass models.

decay, while the α-decay half-life, T_α, becomes much smaller than T_c if the cluster branching ratio is much smaller than zero ($\log_{10} b_c \ll 0$). To find the possible decay modes of a SHN, we calculate the half-lives T_c for several types of clusters emitted from SHN and compare in each case $\log_{10} T_c$ and $\log_{10} T_\alpha$. Clusters with dominant decay mode relative to the corresponding α decay have positive values of $\log_{10} b_c$ or too small negative values.

In the present work we calculate $\log_{10} b_c$ for different cluster emissions from 17 isotopes in the mass number range 294–324 of the SHN with $Z = 124$ and from 12 isotopes in the mass number range 294–312 of the SHN with $Z = 126$. The calculations were performed using four different models, namely, DFM, UDL, Horoi, and UNIV. We explored clusters within the mass number range of $A_c = 18$–126, and subsequently computed the probable cluster decay half-lives for $^{294-324}124$ and $^{294-312}126$ superheavy nuclei (SHN). In our calculations, we employed Q values obtained from the

WS4 mass model [76]. The double folding model failed to calculate the half-lives of clusters with mass number larger than $A_c = 60$, because the Q values exist above the Coulomb barrier. Also, the calculated half-lives by Horoi and UNIV formulas produce $\log_{10} T_c$ with too large positive values, which indicates that the cluster half-lives are large and α decay and SF are the dominant decay modes compared to CR. Moreover, the present study shows that the universal decay law (UDL) produces reasonable values of $\log_{10} T_c$ based on the obtained half-life values. It predicts emission of the isotopes of the heavy clusters Kr, Sr, Zr, Mo, Ru, and Pd.

The probable clusters decay modes with only $\log_{10} b_c > 0$ are represented in Fig. 9 for $Z = 124$ and Fig. 10 for $Z = 126$. Also, the calculated values of $\log_{10} b_c > 0$ and $\log_{10} b_c > 2$ for clusters emissions from $Z = 124$ and $Z = 126$ are listed in Tables I and II, respectively. It is noted that the clusters with $\log_{10} b_c > 0$ are heavy clusters with $Z_c \geqslant 38$; light clusters such as O, N, and even Ca have too large values of T_c
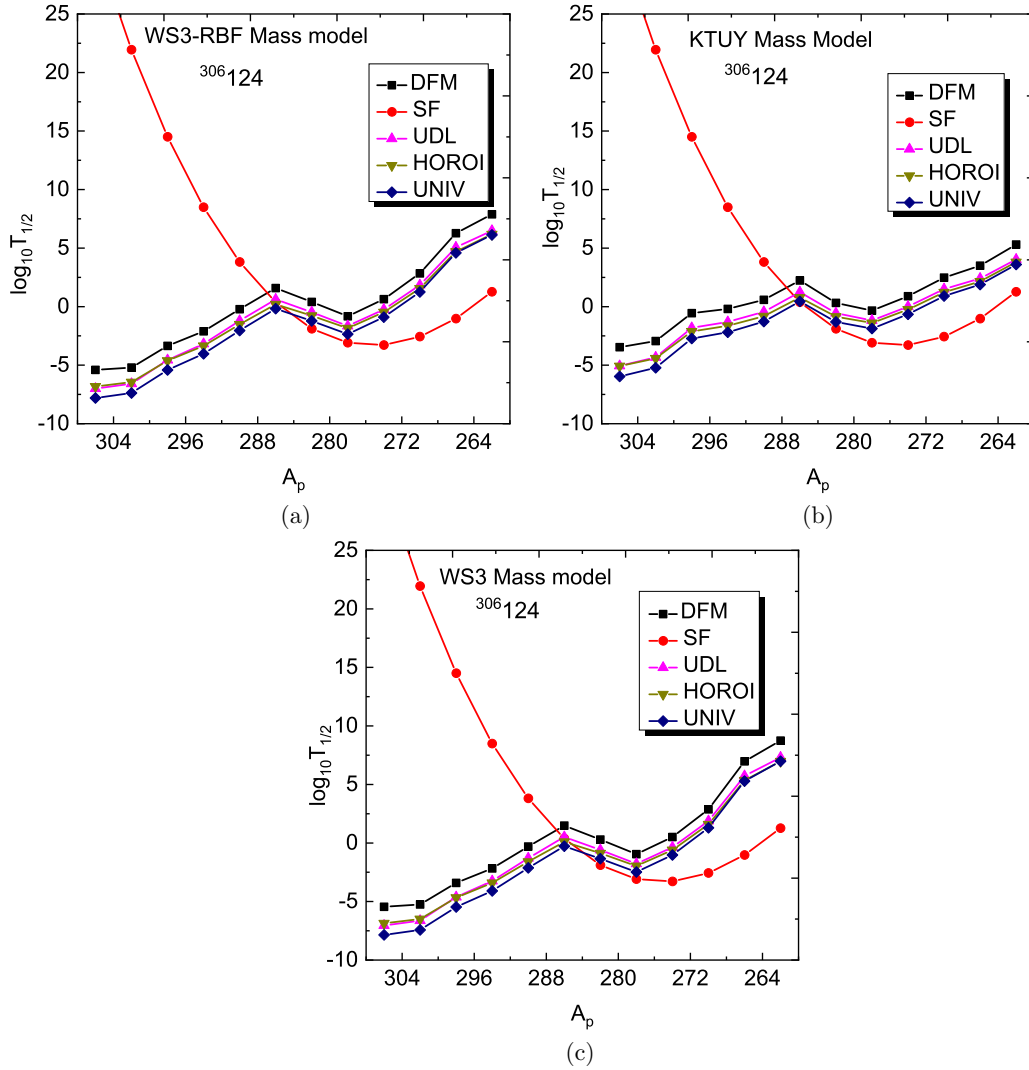
FIG. 8. Comparison of the calculated α-decay half-lives of the isotope $^{306}124$ and products on their α-decay chains using different mass models.

compared to T_α and cannot be emitted. It is interesting to understand, on the basis of energy levels of the mother nuclei, why these types of clusters can be emitted while others cannot. First we try to get an idea on the protons and neutrons levels of the SHN with $Z = 124$. In Ref. [77], the authors considered three double magic superheavy nuclei above the known ^{208}Pb and they derived microscopically the energy levels of protons and neutrons using 12 effective nucleon-nucleon forces. The authors in this reference compared their obtained energy levels for neutrons and protons with the experimental energy levels of ^{208}Pb; the calculated levels from different forces differ slightly but all agree in producing a neutron gap at 126 and a proton gap at 82. Moreover, the four levels before the gaps are exactly the same in all the models and are the same as the experimental levels ($3p_{1/2}, 3p_{3/2}, i_{13/2}, 2d_{5/2}$ for neutrons and $3s_{1/2}, 2d_{3/2}, h_{11/2}, 2d_{5/2}$ for protons) and almost have the same order as the experimental levels.

This study can help us to answer the question, why are these clusters emitted from the SHN and not others? The probable clusters emitted from the isotopes of $^{294-324}124$ and $^{294-312}126$ are the isotopes of the elements Sr, Zr, Mo, Ru, and Pd. These five elements have even Z values. Also the isotopes of the emitted clusters have neutron numbers in the range $46 \leqslant N_c \leqslant 70$. The daughter nuclei have Z_d values ranging from $Z_d = 78$ for Pt to $Z_d = 88$ for Ra.

The largest $\log_{10} b_c$ value in Table I is 7.85 for ^{104}Mo ($Z_c = 42, N_c = 62$) cluster emission from the $^{312}124$ superheavy isotope, leaving the double magic number ^{208}Pb as daughter nucleus. This means that the maximum probability of cluster emission is for the cluster with Z_c and N_c near proton and neutron magic numbers, leaving the double magicity ^{208}Pb nucleus as a daughter. This suggests that the superheavy nuclei follow certain rules governing how their energy levels are arranged when they emit a cluster. Also, the cluster ^{108}Ru ($Z_c = 44, N_c = 64$) from the same SHN isotope leaving ^{204}Hg as the daughter nucleus has a value of $\log_{10} b_c \cong 7.3$. It is known that the upper levels before the proton magic number $Z = 82$ and neutron magic number $N = 126$ are $3s_{1/2}$
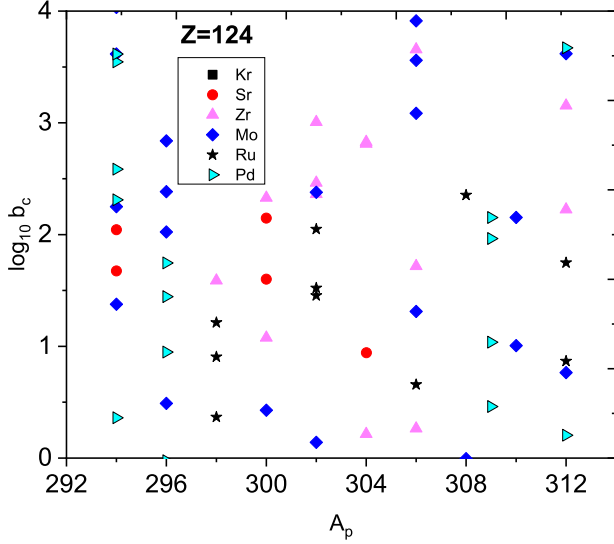
FIG. 9. Decimal logarithm of the branching ratio of the probable CR relative to α decay versus the mass number of the parent nuclei with $Z = 124$.

and $3p_{1/2}$, respectively, each level is filled by two nucleons. Thus, $Z_d = 80$ and $N_d = 124$ are semimagic numbers: below them, all the levels are closed. This means that the most probable cluster emission one leaving the daughter nucleus with double magicity or semimagicity. In this case, the SHN has strong tendency to get rid of the types of cluster whose daughter has double magic or semimagic number and the numbers of protons and/or neutrons in the cluster are semimagic or near magic numbers. It is noted that the neutron numbers $N = 62$, 64, and 66 are found to be semimagic neutron numbers [78]. Other large values of $\log_{10} b_c$ greater than 6 are for ^{106}Mo and ^{106}Ru cluster emissions which leave ^{206}Pb and ^{206}Hg, respectively as daughter nuclei. ^{206}Pb has magic proton number and semimagic neutron number, while ^{206}Hg has quasimagic proton number ($Z_d = 80$) [66] and magic neutron number ($N_d = 126$) [78] and the
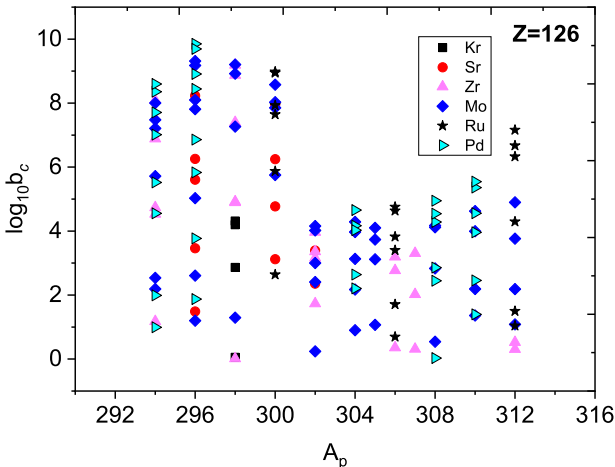
FIG. 10. The same as Fig. 9 but for the isotopes of SHN with $Z = 126$.

clusters have semineutron magicity. The values of $\log_{10} b_c$ greater than 6 are marked by underlined Z_c, N_c, Z_d, N_d, and $\log_{10} b_c$ in Table I. Another large value of branching ratio of about 5 is for the cluster ^{102}Ru from ^{312}124 leading to ^{200}Hg. The value of branching ratio greater than or near 4 is for the clusters ^{88}Sr from the isotopes ^{294}124, $^{94-96}$Mo from the same isotope, ^{100}Mo from ^{306}124, $^{100-102}$Mo from ^{308}124, $^{102-104}$Mo from ^{310}124, and ^{102}Mo from the isotope ^{312}124 of the SHN. These are marked by an asterisk on Z_c, N_c, Z_d, N_d, and $\log_{10} b_c$ values. Except for the decay of ^{294}124 through the emission of a Sr cluster, the above mentioned cluster decays leave the proton magicity lead isotopes as daughter nuclei with neutron numbers ranging from 116–128. For $N_d = 124$, 126, and 128, clear evidence of magicity and quasimagicity is observed in the first two numbers. However, in the case of $N_d = 128$, there are two neutrons occupying the $2g_{9/2}$ level, which has the capacity to accommodate ten neutrons. These two neutrons in the $2g_{9/2}$ level can be easily released.

Table II shows that the SHN with $Z = 126$ tends to emit the same clusters as $Z = 124$. The values of $\log_{10} b_c$ have maxima larger than in Table I, indicating that the isotopes of SHN 126 can emit heavy clusters with larger probability compared to the isotopes of 124. The largest values of $\log_{10} b_c$ are 9.8528 and 9.6946 for Pd ($N_c = 60$ and 58) cluster emission from the ^{296}126 superheavy isotope, leaving the isotopes of Hg ($N_d = 110$ and 112) as daughter nuclei. Note that Hg has proton semimagicity and ^{106,104}Pd are stable nuclei. Also, the stable isotopes of ^{96,94}Mo emitted from the same SHN isotope leaving Pb ($N = 116$ and 118) as daughter isotopes have values of $\log b_c > 9$. For ^{298}126, large values of $\log_{10} b_c > 9$ are found at the doubly magic cluster Zr ($Z_c = 40$, $N_c = 50$) and at Mo ($Z_c = 42$, $N_c = 54$); their residual nuclei are Rn ($Z_d = 86$, $N_d = 122$) and Po ($Z_d = 84$, $N_d = 118$), respectively. The proton and neutron numbers of the last heavy cluster differ slightly from the double magicity cluster ^{90}Zr. From Table II it is noted that larger branching ratios of the probable CR relative to α decay are obtained when the proton and neutron numbers Z_c and N_c of the emitted clusters are equal to or near the proton magic number $Z = 40$ and near to the neutron magicity $N = 50$. Besides, the residual nuclei have proton and neutron numbers in the vicinity of the magic numbers $Z = 82$ and $N = 126$. For example, the values of $\log_{10} b_c$ for the isotopes ^{90}Zr ($N_c = 50$) emitted from ^{294}126 are 8.0919; for the isotopes $^{96-92}$Mo ($N_c = 54$, 52, and 50) they are 7.4751, 8.0038, and 7.2105; and for the isotopes $^{108-102}$Pd ($N_c = 62$, 60, 58, and 56) emitted from the same isotope they are 7.014, 8.3564, 8.5966, and 7.7095. The residual nuclei after the emission of ^{90}Zr, $^{96-92}$Mo, and $^{108-102}$Pd clusters are the isotopes ^{204}Rn ($N_d = 118$), $^{198-202}$Po ($N_d = 114-118$), and $^{186-192}$Hg ($N_d = 106$, 108, 110, and 112), respectively. It is noted that the neutron numbers $N = 58$, 60, 62, 108, and 110 are found to be semimagic neutron numbers in Ref. [78]. The branching values greater than 7 are marked by underlined N_c, N_d, and $\log_{10} b_c$. Moreover, the branching values in the range of $5 \leqslant \log b_c \leqslant 7$ are marked by asterisks on N_c, N_d, and $\log_{10} b_c$ in Table II.

From Tables I and II, it is noted that the repetition of Mo and Ru clusters in the large branching ratio values indicates

TABLE I. The probable clusters emitted and their residual nuclei for all considered isotopes of $Z = 124$.

Parent	Cluster	Z_c	N_c	Daughter	Z_d	N_d	$\log_{10} b_c$
$^{294}124$	Sr	38*	(52, 50*, 48)	Ra	86*	(118, 120*,122)	(2.0436, 4.2334*, 1.6751)
	Mo	42*	(58, 56, 54*, 52, 50)	Pb	82*	(112, 114, 116*, 118, 120)	(1.3763,3.6169,4.4453*,4.0327, 2.2501)
	Pd	46	(64, 62, 60, 58, 56)	Pt	78	(106, 108, 110, 112, 114)	(2.3108, 3.5456, 3.6152, 2.5846, 0.3611)
$^{296}124$	Mo	42	(58, 56, 54, 52)	Pb	82	(114, 116, 118, 120)	(0.4898, 2.3837, 2.8384, 2.0233)
	Pd	46	(64, 62, 60)	Pt	78	(108, 110, 112)	(0.9482, 1.7462, 1.4441)
$^{298}124$	Zr	40	50	Po	84	124	1.5887
	Ru	44	(60, 58, 56)	Hg	80	(114, 116, 118)	(0.9063, 1.2129, 0.3676)
$^{300}124$	Sr	38	(52, 50)	Ra	86	(124, 126)	(1.6022, 2.1495)
	Zr	40	(52,50)	Po	84	(124,126)	(2.3294, 1.0775)
	Mo	42	52	Pb	82	124	0.4285
$^{302}124$	Zr	40	(56, 54, 52)	Po	84	(122,124,126)	(2.3622, 3.0067, 2.4639)
	Mo	42	(54, 52)	Pb	82	(124, 126)	(2.3782, 0.1411)
	Ru	44	(62, 60, 58)	Hg	80	(116, 118, 120)	(1.5215, 2.0491, 1.4546)
$^{304}124$	Sr	38	54	Ra	86	126	0.9437
	Zr	40	(58, 56, 54)	Po	84	(122, 124, 126)	(0.2156, 2.8282, 2.8128)
$^{306}124$	Zr	40	(58, 56, 54)	Po	84	(124, 126, 128)	(1.7175, 3.6573, 0.2643)
	Mo	42	(62, 60, 58, 56)	Pb	82	(120, 122, 124, 126)	(1.3123, 3.0859, 3.9128, 3.5599)
	Ru	44	58	Hg	80	124	0.6581
$^{308}124$	Mo	42*	(60*, 58)	Pb	82*	(124*, 126)	(4.2763*, 4.503)
	Ru	44	60	Hg	80	124	2.3535
	Pd	46	(70,,68, 66,64)	Pt	78	(114, 116, 118,120)	(0.3543, 1.9995, 2.4123, 1.5466)
$^{309}124$	Pd	46	(70, 68, 66, 64)	Pt	78	(115, 117, 119, 121)	(0.4614, 1.964, 2.1519, 1.0371)
$^{310}124$	Mo	42*	(64, 62*, 60*, 58)	Pb	82*	(122, 124*, 126*, 128)	(2.1531, 4.2823*, 4.4981*, 1.0059)
$^{312}124$	Zr	40	(62, 60)	Po	84	(126, 128)	(3.154, 2.2249)
	Mo	42*	(66, <u>64</u>, <u>62</u>, 60*, 58)	Pb	82*	(122, <u>124</u>, <u>126</u>, 128*, 130)	(3.6182, <u>6.7848</u>, <u>7.8532</u>, 4.8453*, 0.7646)
	Ru	44*	(70, 68*, <u>66</u>, <u>64</u>, <u>62</u>, 60)	Hg	80*	(118, 120*, <u>122</u>, <u>124</u>, <u>126</u>, 128)	(1.7485, 4.9795*, <u>6.7088</u>, <u>7.264</u>, <u>6.1147</u>, 0.8677)
	Pd	46	(64, 62)	Pt	78	(124, 126)	(3.6712, 0.2048)

that $Z_c = 42$ and 44 are stable proton numbers. This is clear from the stability of the even mass number isotopes of element Mo in the periodic table. Additional evidence supporting the proton numbers $Z_c = 42$ and $Z_c = 44$ is shown in the level arrangements of the two superheavy nuclei ($Z_p = 120$ and $Z_p = 126$) presented in Ref. [62]. The proton level arrangements of SHN $Z = 120$ and 126 show that the proton levels below the $Z = 126$ gap are $3p_{1/2}$, $3p_{3/2}$, $2f_{5/2}$, $2f_{7/2}$, $i_{13/2}$, and $h_{9/2}$; these six levels are filled completely by 44 protons and, if the upper level ($3p_{1/2}$) is absent, the remaining levels will be completely filled by 42 protons. This means that the cluster emitted picks up the upper filled proton levels from the SHN to form its protons. Also, these large $\log_{10} b_c$ values correspond to magic or semimagic neutron numbers of the daughters and correspond to $N_c = 62$ and 64 for Mo. Thus the stability of protons in the two clusters Mo and Ru is the reason for their repetition in Tables I and II. A large branching ratio, which measures the probability of cluster emission, does not depend only on the proton stability of the cluster, but it is one factor among four others governing the value of $\log_{10} b_c$. The first is the neutron stability of the cluster. For example, $\log_{10} b_c \cong 4.5$ for the decay $^{306}124 \rightarrow {}^{100}\text{Mo} + {}^{208}\text{Pb}$; the number of neutrons in the cluster is $N_c = 58$ which is quasineutron magicity as found in Ref. [78] based on the study of α-emission half-life time variation with daughter nucleus neutron number N_d. At magic or semimagic neutron numbers,

$\log_{10} T_{1/2}$ shows a minimum or dip in its behavior with N_d. Other factors governing the stability and influencing the value of $\log_{10} b_c$ include the stability of protons and neutrons in the daughter nucleus. Table I shows that $\log_{10} b_c$ has large values for $^{206-208}\text{Pb}$ and $^{200-206}\text{Hg}$ compared to ^{202}Pb, for example, since the latter has four neutrons in the unfilled $2f_{5/2}$ level below the $3p_{1/2}$ neutron level.

IV. SUMMARY AND CONCLUSION

A comparison between spontaneous fission and α-decay half-lives of SHN $Z = 124$ and 126 in the mass number range $292 \leqslant A \leqslant 314$ has been performed. The double-folding (DFM) model derived from the Michigan three-range Yukawa-Reid NN interaction with zero range exchange part as well as the universal decay law (UDL) formula, the scaling law of Horoi, and the UNIV formula are utilized to compute the α-decay half-lives. For spontaneous fission (SF) half-lives, we utilize the semi empirical relation of Xu *et al.* [39]. The study of the variation of $\log_{10} T_{1/2}$ against parent nucleus mass numbers of α-decay chains of the considered SHN show some maxima of $\log_{10} T_{1/2}$ at specific proton and neutron numbers. These numbers correspond to magic proton number (such as $Z_P = 114$) or magic neutron number (such as $N_P = 184$) or even to nucleon numbers near magicity (such as $Z_P = 106$ and 116 and $N_P = 150, 164, 170, 174,$ and 178).

TABLE II. The same as Table I but for the isotopes of $Z = 126$.

Parent	Cluster	Z_c	N_c	Daughter	Z_d	N_d	$\log_{10} b_c$
$^{294}126$	Zr	40	(54,52*,<u>50</u>,48)	Rn	86	(114,116*,<u>118</u>,120)	(4.5324, 6.8851*, <u>8.0919</u>, 4.735)
	Mo	42	(58,56*,<u>54</u>,52,50,48)	Po	84	(110,112*,<u>114</u>, <u>116</u>,118,1120)	(2.5362, 5.7151*, <u>7.4751</u>, <u>8.0038</u>, 7.2105, 2.1892)
	Pd	46	(64,<u>62</u>,<u>60</u>,<u>58</u>,<u>56</u>, 54*)	Hg	80	(104,<u>106</u>,<u>108</u>,<u>110</u>,<u>112</u>,114*)	(4.5546, <u>7.014</u>, <u>8.3564</u>, <u>8.5966</u>, <u>7.7095</u>, 5.519*)
$^{296}126$	Sr	38	(52*,<u>50</u>,48*,46)	Ra	88	(118*,<u>120</u>, 122*, 124)	(5.605*, <u>8.2341</u>, 6.2605*, 3.4625)
	Mo	42	(58*,<u>56</u>,<u>54</u>,<u>52</u>,<u>50</u>,48)	Po	84	(112*, <u>114</u> <u>116</u>, <u>118</u>, <u>120</u>,122)	(5.0269*, <u>7.812</u>, <u>9.1758</u>, <u>9.3133</u>, <u>8.0971</u>, 2.6089)
	Pd	46	(66,64*,<u>62</u>,<u>60</u>,<u>58</u>,<u>56</u>,54*)	Hg	80	(104,106*,<u>108</u>,<u>110</u>,<u>112</u>,<u>114</u>,116*)	(3.7718, 6.8592*, <u>8.9081</u>, <u>9.8528</u>, <u>9.6946</u>, <u>8.4442</u>, 5.8325*)
$^{298}126$	Kr	36	(48,46,44)	Th	90	(124,126,128)	(4.1979,4.3145,2.8635)
	Zr	40	(56,<u>54</u>,<u>52</u>,<u>50</u>,48)	Rn	86	(116,<u>118</u>,<u>120</u>,<u>122</u>, 124)	(4.9175, <u>7.3995</u>, <u>8.8742</u>, <u>9.1924</u>, 4.8961)
	Mo	42	(<u>54</u>,<u>52</u>,<u>50</u>)	Po	84	(<u>118</u> <u>120</u>,<u>122</u>)	(<u>9.2049</u>, <u>8.9204</u>, <u>7.2648</u>)
$^{300}126$	Sr	38	(54,52*,<u>50</u>,48)	Ra	88	(120,122*,<u>124</u>,126)	(3.1204, 6.251*,<u>7.9609</u>,4.7729)
	Mo	42	(<u>56</u>,<u>54</u>,<u>52</u>,50*)	Po	84	(<u>118</u>,<u>120</u>,<u>122</u>,124*)	(<u>8.0297</u>, <u>8.5754</u>,<u>7.8536</u>, 5.753*)
	Ru	44	(64,62*,<u>60</u>,<u>58</u>,<u>56</u>,<u>54</u>)	Pb	82	(110,112*,<u>114</u>,<u>116</u>, <u>118</u>, <u>120</u>)	(2.6399,5.8721*, <u>7.9289</u>, <u>8.9818</u>, <u>8.9459</u>,<u>7.6463</u>)
$^{302}126$	Sr	38	(50,48)	Ra	88	(124,126)	(2.3614,3.3947)
	Zr	40	(54,52,50)	Rn	86	(122,124,126)	(3.3588,3.967,3.1634)
	Mo	42	(58,56,54,52)	Po	84	(118,120, 122,124)	(2.4086,4.0216,4.1581,3.0003)
$^{304}126$	Mo	42	(58,56,54,52)	Po	84	(120, 122,124,126)	(3.1296,4.287,3.9723,2.1738)
	Pd	46	(66,64,62,60,58)	Hg	80	(112,114,116,118,120)	(2.6385,4.166,4.6565,4.0271,2.2063)
$^{305}126$	Mo	42	(58,56,54)	Po	84	(121,123,125)	(3.1164,4.1017,3.7362)
$^{306}126$	Zr	40	(56,54)	Rn	86	(124,126)	(2.7694,3.1937)
	Ru	44	(62,60,58,56)	Pb	82	(118,120,122,124)	(3.8222,4.7547,4.6354, 3.4017)
$^{307}126$	Zr	40	(56,54)	Rn	86	(125,127)	(3.3073,2.0206)
$^{308}126$	Mo	42	(60,58,56)	Po	84	(122,124,126)	(2.834,4.1197,4.1705)
	Pd	46	(68,66,64,62,60)	Hg	80	(114,116,118,120,122)	(2.4478,4.2822,4.9459,4.542, 2.8584)
$^{310}126$	Mo	42	(62,60,58)	Po	84	(122,124,126)	(2.188,3.9964,4.6248)
	Pd	46	(68,66*,<u>64</u>*,62,60)	Hg	80	(116,118*,<u>120</u>*,122, 124)	(3.9596,5.3589*,5.5433*, 4.5582,2.458)
$^{312}126$	Mo	42	(62,60,58)	Po	84	(124,126,128)	(3.7652,4.8995,2.1875)
	Ru	44	(66,64*,<u>62</u>,60*)	Pb	82	(120,122*,<u>124</u>,126*)	(4.2929,6.3272*,<u>7.1591</u>, 6.6725*)

Moreover, we studied the most probable heavy cluster radioactivity (CR) in the mass number range $A_c = 18$–126 from $^{294-324}124$ and $^{294-312}126$ by calculating cluster decay half-lives ($\log_{10} T_c$) using the same four models of α-decay half-lives. The values of $\log_{10} T_c$ is then compared to the α-decay half-lives using the branching ratio quantity ($\log_{10} b_c$) of CR relative to the corresponding α decay. The study shows that the universal decay law (UDL) is the only one that produces reasonable values of $\log_{10} T_c$. Within this model, six heavy cluster emissions, namely, Kr, Sr, Zr, Mo, Ru, and Pd

emissions are observed from both SHN $Z = 124$ and 126 as dominant decay modes relative to α decay. Also, we found that clusters with dominant decay mode relative to the corresponding α decay have positive values of $\log_{10} b_c$ or too small negative values. Additionally, larger branching ratios of the probable CR relative to α decay are obtained when the clusters have proton and/or neutron numbers corresponding to magic or near magic numbers, and leaving a double magicity or semimagicity nucleus as a daughter.

[1] Y. T. Oganessian and V. K. Utyonkov, Rep. Prog. Phys. **78**, 036301 (2015).

[2] Y. T. Oganessian, A. Sobiczewski, and G. M. Ter-Akopian, Phys. Scr. **92**, 023003 (2017).

[3] N. T. Brewer, V. K. Utyonkov, K. P. Rykaczewski, Y. T. Oganessian, F. S. Abdullin, R. A. Boll, D. J. Dean, S. N. Dmitriev, J. G. Ezold, L. K. Felker, R. K. Grzywacz, M. G. Itkis, N. D. Kovrizhnykh, D. C. McInturff, K. Miernik, G. D. Owen, A. N. Polyakov, A. G. Popeko, J. B. Roberto, A. V. Sabel'nikov *et al.*, Phys. Rev. C **98**, 024317 (2018).

[4] D. N. Poenaru and R. A. Gherghescu, Europhys. Lett. **124**, 52001 (2018).

[5] V. K. Utyonkov, N. T. Brewer, Y. T. Oganessian, K. P. Rykaczewski, F. S. Abdullin, S. N. Dmitriev, R. K. Grzywacz, M. G. Itkis, K. Miernik, A. N. Polyakov, J. B. Roberto, R. N. Sagaidak, I. V. Shirokovsky, M. V. Shumeiko, Y. S. Tsyganov,

A. A. Voinov, V. G. Subbotin, A. M. Sukhov, A. V. Karpov, A. G. Popeko *et al.*, Phys. Rev. C **97**, 014320 (2018).

[6] M. Ismail and A. Adel, J. Phys. G: Nucl. Part. Phys. **46**, 075105 (2019).

[7] M. Ismail and A. Adel, Phys. Rev. C **101**, 024607 (2020).

[8] Z. Wang, Z. Ren, and D. Bai, Phys. Rev. C **101**, 054310 (2020).

[9] Y. T. Oganessian and K. P. Rykaczewski, Phys. Today **68**(8), 32 (2015).

[10] D. Ackermann, Nucl. Phys. A **787**, 353 (2007).

[11] K. Morita, Nucl. Phys. A **944**, 30 (2015).

[12] Y. T. Oganessian, V. K. Utyonkov, Y. V. Lobanov, F. S. Abdullin, A. N. Polyakov, R. N. Sagaidak, I. V. Shirokovsky, Y. S. Tsyganov, A. A. Voinov, G. G. Gulbekian, S. L. Bogomolov, B. N. Gikal, A. N. Mezentsev, S. Iliev, V. G. Subbotin, A. M. Sukhov, K. Subotic, V. I. Zagrebaev, G. K. Vostokin, M. G. Itkis *et al.*, Phys. Rev. C **74**, 044602 (2006).

[13] J. Khuyagbaatar, A. Yakushev, C. E. Düllmann, D. Ackermann, L.-L. Andersson, M. Asai, M. Block, R. A. Boll, H. Brand, D. M. Cox, M. Dasgupta, X. Derkx, A. Di Nitto, K. Eberhardt, J. Even, M. Evers, C. Fahlander, U. Forsberg, J. M. Gates, N. Gharibyan *et al.*, Phys. Rev. C **102**, 064602 (2020).

[14] D. N. Poenaru, R. A. Gherghescu, and W. Greiner, J. Phys. G: Nucl. Part. Phys. **39**, 015105 (2012).

[15] D. N. Poenaru, R. A. Gherghescu, and W. Greiner, Phys. Rev. C **85**, 034615 (2012).

[16] D. N. Poenaru, H. Stöcker, and R. A. Gherghescu, Eur. Phys. J. A **54**, 14 (2018).

[17] G. Royer and R. Moustabchir, Nucl. Phys. A **683**, 182 (2001).

[18] H. F. Zhang and G. Royer, Phys. Rev. C **76**, 047304 (2007).

[19] D. Ni and Z. Ren, Phys. Rev. C **81**, 024315 (2010).

[20] Y. Qian and Z. Ren, Eur. Phys. J. A **52**, 68 (2016).

[21] A. Adel and T. Alharbi, Nucl. Phys. A **958**, 187 (2017).

[22] M. Ismail and A. Adel, Phys. Rev. C **97**, 044301 (2018).

[23] K. P. Santhosh, R. K. Biju, and S. Sahadevan, Nucl. Phys. A **838**, 38 (2010).

[24] K. P. Santhosh, B. Priyanka, and M. S. Unnikrishnan, Nucl. Phys. A **889**, 29 (2012).

[25] K. P. Santhosh and C. Nithya, Phys. Rev. C **97**, 064616 (2018).

[26] K. P. Santhosh, C. Nithya, H. Hassanabadi, and D. T. Akrawy, Phys. Rev. C **98**, 024625 (2018).

[27] C. Qi, F. R. Xu, R. J. Liotta, and R. Wyss, Phys. Rev. Lett. **103**, 072501 (2009).

[28] C. Qi, F. R. Xu, R. J. Liotta, R. Wyss, M. Y. Zhang, C. Asawatangtrakuldee, and D. Hu, Phys. Rev. C **80**, 044326 (2009).

[29] D. N. Poenaru, R. A. Gherghescu, and W. Greiner, Phys. Rev. C **83**, 014601 (2011).

[30] M. Horoi, J. Phys. G: Nucl. Part. Phys. **30**, 945 (2004).

[31] D. Ni, Z. Ren, T. Dong, and C. Xu, Phys. Rev. C **78**, 044310 (2008).

[32] C. Qi, R. Liotta, and R. Wyss, Prog. Part. Nucl. Phys. **105**, 214 (2019).

[33] M. Warda and L. M. Robledo, Phys. Rev. C **84**, 044608 (2011).

[34] C. Xu, G. Röpke, P. Schuck, Z. Ren, Y. Funaki, H. Horiuchi, A. Tohsaki, T. Yamada, and B. Zhou, Phys. Rev. C **95**, 061306(R) (2017).

[35] S. Yang, C. Xu, G. Röpke, P. Schuck, Z. Ren, Y. Funaki, H. Horiuchi, A. Tohsaki, T. Yamada, and B. Zhou, Phys. Rev. C **101**, 024316 (2020).

[36] Z. Wang and Z. Ren, Phys. Rev. C **108**, 024306 (2023).

[37] M. Wang, W. J. Huang, F. G. Kondev, G. Audi, and S. Naimi, Chin. Phys. C **45**, 030003 (2021).

[38] Y. Gao, J. Cui, Y. Wang, and J. Gu, Sci. Rep. **10**, 9119 (2020).

[39] C. Xu, Z. Ren, and Y. Guo, Phys. Rev. C **78**, 044329 (2008).

[40] B. Buck, J. C. Johnston, A. C. Merchant, and S. M. Perez, Phys. Rev. C **53**, 2841 (1996).

[41] M. Ismail and A. Adel, Phys. Rev. C **89**, 034617 (2014).

[42] R. E. Langer, Phys. Rev. **51**, 669 (1937).

[43] M. Wang, G. Audi, A. H. Wapstra, F. G. Kondev, M. MacCormick, X. Xu, and B. Pfeiffer, Chin. Phys. C **36**, 1603 (2012).

[44] G. R. Satchler and W. G. Love, Phys. Rep. **55**, 183 (1979).

[45] M. Ismail, A. Y. Ellithi, M. M. Botros, and A. Adel, Phys. Rev. C **81**, 024602 (2010).

[46] C. Xu and Z. Ren, Phys. Rev. C **74**, 014304 (2006).

[47] K. Wildermuth and Y. C. Tang, *A Unified Theory of the Nucleus* (Academic, New York, 1977).

[48] Y. Qian, Z. Ren, and D. Ni, Phys. Rev. C **94**, 024315 (2016).

[49] M. Ismail, W. M. Seif, and A. Abdurrahman, Phys. Rev. C **94**, 024316 (2016).

[50] D. Ni and Z. Ren, Phys. Rev. C **82**, 024311 (2010).

[51] W. M. Seif, M. Ismail, A. I. Refaie, and L. H. Amer, J. Phys. G: Nucl. Part. Phys. **43**, 075101 (2016).

[52] C. Xu and Z. Ren, Nucl. Phys. A **753**, 174 (2005).

[53] C. Xu and Z. Ren, Nucl. Phys. A **760**, 303 (2005).

[54] Z. Wang, D. Bai, and Z. Ren, Phys. Rev. C **105**, 024327 (2022).

[55] Z. Wang and Z. Ren, Phys. Rev. C **106**, 024311 (2022).

[56] M. Ismail, W. M. Seif, W. M. Tawfik, and A. M. Hussein, Ann. Phys. (NY) **406**, 1 (2019).

[57] W. M. Seif, J. Phys. G: Nucl. Part. Phys. **40**, 105102 (2013).

[58] W. M. Seif, M. Ismail, and E. T. Zeini, J. Phys. G: Nucl. Part. Phys. **44**, 055102 (2017).

[59] M. Ismail and A. Adel, Int. J. Mod. Phys. E **29**, 2050065 (2020).

[60] S. Ćwiok, S. Hofmann, and W. Nazarewicz, Nucl. Phys. A **573**, 356 (1994).

[61] J. H. Hamilton, S. Hofmann, and Y. T. Oganessian, J. Phys.: Conf. Ser. **580**, 012019 (2015).

[62] M. Bender, K. Rutz, P.-G. Reinhard, J. A. Maruhn, and W. Greiner, Phys. Rev. C **60**, 034304 (1999).

[63] M. Ismail, W. M. Seif, A. Adel, and A. Abdurrahman, Nucl. Phys. A **958**, 202 (2017).

[64] S. G. Nilsson, C. F. Tsang, A. Sobiczewski, Z. Szymański, S. Wycech, C. Gustafson, I.-L. Lamm, P. Möller, and B. Nilsson, Nucl. Phys. A **131**, 1 (1969).

[65] S. G. Nilsson, S. G. Thompson, and C. F. Tsang, Phys. Lett. B **28**, 458 (1969).

[66] M. Ismail, A. Y. Ellithi, A. Adel, and H. Anwer, Chin. Phys. C **40**, 124102 (2016).

[67] S. Ćwiok, J. Dobaczewski, P.-H. Heenen, P. Magierski, and W. Nazarewicz, Nucl. Phys. A **611**, 211 (1996).

[68] A. V. Afanasjev, Phys. Scr. **T125**, 62 (2006).

[69] V. Y. Denisov, Phys. At. Nucl. **70**, 244 (2007).

[70] R. K. Gupta, S. K. Patra, and W. Greiner, Mod. Phys. Lett. A **12**, 1727 (1997).

[71] Y. Z. Wang, S. J. Wang, Z. Y. Hou, and J. Z. Gu, Phys. Rev. C **92**, 064301 (2015).

[72] N. Wang and M. Liu, Phys. Rev. C **84**, 051303(R) (2011).

[73] M. Liu, N. Wang, Y. Deng, and X. Wu, Phys. Rev. C **84**, 014333 (2011).

[74] H. Koura, T. Tachibana, M. Uno, and M. Yamada, Prog. Theor. Phys. **113**, 305 (2005).

[75] D. N. Poenaru, R. A. Gherghescu, and W. Greiner, Phys. Rev. Lett. **107**, 062503 (2011).

[76] N. Wang, M. Liu, X. Wu, and J. Meng, Phys. Lett. B **734**, 215 (2014).

[77] T. Bürvenich, K. Rutz, M. Bender, P.-G. Reinhard, J. A. Maruhn, and W. Greiner, Eur. Phys. J. A **3**, 139 (1998).

[78] M. Ismail, S. G. Abd-Elnasser, H. M. Elsharkawy, and I. A. M. Abdul-Magead, Nucl. Phys. A **1029**, 122547 (2023).